A&A 525, A68 (2011)
DOI: 10.1051/0004-6361/201015276

Astronomy & Astrophysics

Transiting exoplanets from the *CoRoT* space mission⋆

XV. CoRoT-15b: a brown-dwarf transiting companion

F. Bouchy[1,2], M. Deleuil[3], T. Guillot[4], S. Aigrain[5], L. Carone[6], W. D. Cochran[7], J. M. Almenara[8,9], R. Alonso[10], M. Auvergne[11], A. Baglin[11], P. Barge[3], A. S. Bonomo[3], P. Bordé[12], Sz. Csizmadia[13], K. De Bondt[3], H. J. Deeg[8,9], R. F. Díaz[1], R. Dvorak[14], M. Endl[7], A. Erikson[13], S. Ferraz-Mello[15], M. Fridlund[16], D. Gandolfi[16,17], J. C. Gazzano[3], N. Gibson[5], M. Gillon[18], E. Guenther[17], A. Hatzes[17], M. Havel[4], G. Hébrard[1], L. Jorda[3], A. Léger[12], C. Lovis[10], A. Llebaria[3], H. Lammer[19], P. J. MacQueen[7], T. Mazeh[20], C. Moutou[3], A. Ofir[20], M. Ollivier[12], H. Parviainen[8,9], M. Pätzold[6], D. Queloz[10], H. Rauer[13,21], D. Rouan[11], A. Santerne[3], J. Schneider[22], B. Tingley[8,9], and G. Wuchterl[17]

(Affiliations can be found after the references)

Received 24 June 2010 / Accepted 30 September 2010

ABSTRACT

We report the discovery by the *CoRoT* space mission of a transiting brown dwarf orbiting a F7V star with an orbital period of 3.06 days. CoRoT-15b has a radius of $1.12^{+0.30}_{-0.15}$ $R_{\rm Jup}$ and a mass of 63.3 ± 4.1 $M_{\rm Jup}$, and is thus the second transiting companion lying in the theoretical mass domain of brown dwarfs. CoRoT-15b is either very young or inflated compared to standard evolution models, a situation similar to that of M-dwarf stars orbiting close to solar-type stars. Spectroscopic constraints and an analysis of the lightcurve imply a spin period in the range 2.9–3.1 days for the central star, which is compatible with a double-synchronisation of the system.

Key words. brown dwarfs – stars: low-mass – planetary systems – techniques: photometric – techniques: radial velocities – techniques: spectroscopic

1. Introduction

The *CoRoT* space mission (Baglin et al. 2009), which has been in operation since the start of 2007 and extended to the end of 2013, is designed to identify transiting exoplanets. A natural consequence of this mission is that any object Jupiter-size or lower that transits its host star can be detected. This includes stellar and sub-stellar companions such as M-dwarfs and brown dwarfs (BDs). In the mass-radius diagram of transiting companions orbiting solar-type stars, there has been until now only one known brown dwarf, CoRoT-3b (Deleuil et al. 2008), located in the gap in mass between planetary and low-mass star companions[1]. Determining the physical properties of these objects is fundamental to understanding the link between the population of planets and low-mass stars and distinguishing the formation and evolution processes of the two populations.

In this paper, we report the discovery by *CoRoT* of a new transiting brown-dwarf, which has been established and characterized thanks to ground-based follow-up observations. CoRoT-15b, with an estimated radius of 1.12 $R_{\rm Jup}$ and an estimated mass of 63.3 $M_{\rm Jup}$, orbits in 3.06 days an F-type dwarf of solar metallicity.

2. *CoRoT* observations

SRa02 was the seventh field observed by *CoRoT* in the second year after its launch. It corresponds to the third short run and was located towards the so-called Galactic anti-center direction. This run started on 2008 October 11 and ended on 2008 November 12, constituting of a total of 31.7 days of almost-continuous observations.

More than 30 multi-transiting candidates for planets were found among the 10 265 targets of the SRa02 field. About half of them were clearly identified as binaries from the light-curve analysis and around a tenth of high priority planet-size candidates were selected in this short run including SRa02_E1_4106, which we afterwards call CoRoT-15. The various ID of this target, including coordinates and magnitudes are listed in Table 1.

3. *CoRoT* light-curve analysis

CoRoT-15, with an estimated *V* magnitude close to 16, is among the faintest of the stars observed by *CoRoT*. In this magnitude domain, the signal is not sufficient to allow us to divide the photometric aperture into three colors and the extracted lightcurve, also called a white lightcurve, is monochromatic (Llebaria & Guterman 2006). The sampling data rate was at 512 s during the entire run and it was not oversampled to 32 s since this candidate was not identified with the alarm mode (Surace et al. 2008). Figure 1 shows the lightcurve of CoRoT-15 produced by the N2 data levels pipeline. This lightcurve is quite noisy and is affected by several high-energy-particle impacts that cause hot pixels, as well as possibly stellar variability.

⋆ The *CoRoT* space mission, launched on December 27th 2006, has been developed and is operated by CNES, with the contribution of Austria, Belgium, Brazil, ESA (RSSD and Science Programme), Germany, and Spain. Observations made with HARPS spectrograph at ESO La Silla Observatory (184.C-0639).

[1] After submission of our manuscript, Johnson et al. (2010) reported the discovery of the transiting brown dwarf LHS6343C with a radius of 0.996 ± 0.026 $R_{\rm Jup}$ and a mass of 70.6 ± 2.7 $M_{\rm Jup}$.

Table 1. IDs, coordinates, and magnitudes.

CoRoT window ID	SRa02_E1_4106
CoRoT ID	221686194
USNO-B1 ID	0961–0097866
2MASS ID	06282781+0611105
RA (J2000)	06:28:27.82
Dec (J2000)	+06:11:10.47
B1[a]	16.85
B2[a]	16.59
R1[a]	15.47
R2[a]	15.43
I[a]	14.83
J[b]	13.801 ± 0.026
H[b]	13.423 ± 0.037
K[b]	13.389 ± 0.050

Notes. [(a)] From USNO-B1 catalog ; [(b)] from 2MASS catalog .

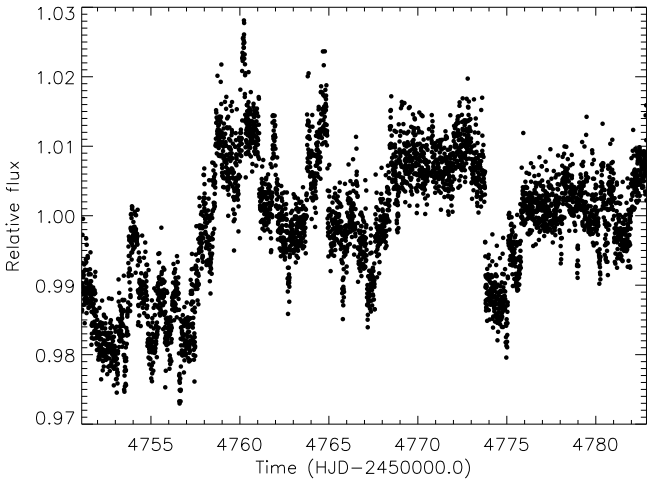

Fig. 1. Raw light curve of CoRoT-15.

A first analysis of the lightcurve (LC), based on a trapezoidal fit to each individual transit, reveals periodic transits of depth 0.68% and a period of 3.0608 ± 0.0008 days.

Since the *CoRoT* lightcurve is relatively noisy, no meaningful limits to either the visible-light albedo of the companion nor its dayside surface temperature could be established.

From the raw lightcurve, we tried to estimate the stellar rotation period. We filtered out variations with timescales shorter than 15 data points (~2.13 h) to reduce the sensitivity to the satellite orbital effects and other short-term variations, and we then removed the transits. The computed LS periodogram appears to be quite noisy and affected by low-level discontinuities in the lightcurve. There is tentative evidence of a rotational modulation at either 2.9, 3.1, or 6.3 days in the light curve, but the data does not enable us to estimate the period more precisely or to distinguish between these values.

4. Ground-based observations

4.1. Ground-based photometric follow-up

Ground-based photometry was performed with the aim of refining the target ephemeris to verify that none of its closest contaminant stars correspond to an eclipsing binary and determine the contamination from nearby stars inside *CoRoT*'s photometric aperture mask (Deeg et al. 2009). CoRoT-15 was observed during a transit event on 2010 January 13 by performing time-series

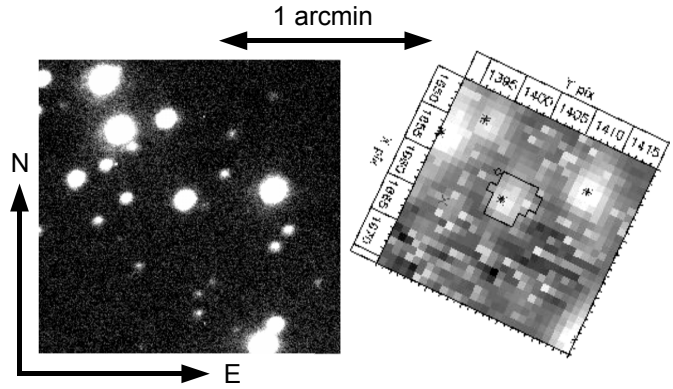

Fig. 2. The image of the sky around CoRoT-15 (star in the center). *Left*: *R*-filter image with a resolution of 1.7″ taken with the IAC80 telescope. *Right*: image taken by *CoRoT*, at the same scale and orientation. The jagged outline in its center is the photometric aperture mask; indicated are also *CoRoT*'s *x* and *y* image coordinates and positions of nearby stars which are in the Exo-Dat (Deleuil et al. 2009) database.

photometry at the IAC80 telescope, from HJD 2455209.480 to .676. The resultant lightcurve was not sufficiently precise to identify the expected transit of the target because of the photometric errors introduced by the presence of thin cirrus. However, the absence of large brightness variations in the neighboring stars allowed us to exclude nearby eclipsing binaries as a source of the signals observed by *CoRoT*. The contamination factor was derived from the measured distance and brightness of the nearby stars for a subset of these IAC80 *R*-filter images obtained with the best seeing of that night (1.7 arcsec). Ten nearby stars were identified, with six of them contaminating the *CoRoT* window aperture at a flux level that amounts to 1.9 ± 0.3% of the main target flux. Furthermore, we verified that none of the known nearby stars is bright enough to be contaminating eclipsing binaries. The image of the sky around CoRoT-15 is shown in Fig. 2.

4.2. Radial velocity follow-up

Radial velocity (RV) observations of CoRoT-15 were performed with the HARPS spectrograph (Mayor et al. 2003) mounted at the 3.6-m ESO telescope (Chile) as part of the ESO large program 184.C-0639 and with the HIRES spectrograph (Vogt et al. 1994) mounted at the 10-m Keck-1 telescope as part of NASA's key science project to support the *CoRoT* mission.

HARPS was used with the observing mode obj_AB, without simultanenous thorium in order to monitor the Moon background light on the second fiber. The exposure time was set to 1 h. A set of 9 spectra was recorded between 2009 November 24 and 2010 February 21. We reduced HARPS data and computed RVs with the pipeline based on cross-correlation techniques (Baranne et al. 1996; Pepe et al. 2002). The signal-to-noise ratio (SNR) per pixel at 550 nm is in the range from 3 to 7.8 for this faint target, which corresponds to the faint end in magnitude for HARPS follow-up observations. Radial velocities were obtained by performing weighted cross-correlation with a numerical G2 mask.

HIRES observations were performed with the red cross-disperser and the I_2-cell to measure RVs. We used the 0.861″ wide slit that leads to a resolving power of $R \approx 45\,000$. The contamination of the HIRES spectra by scattered moonlight was significant for this faint target, but the 7″ tall decker allowed us to properly correct for the background light. Three spectra without the iodine cell were obtained on 2010 December 2 and January 9.

Table 2. Radial velocity measurements of CoRoT-15 obtained by HARPS and HIRES. BJD is the barycentric Julian date.

BJD –2 400 000	RV [km s^{-1}]	$\pm 1\sigma$ [km s^{-1}]
HARPS 3.6-m ESO		
55159.81312	9.944	0.308
55169.77922	2.107	0.315
55235.60498	2.849	0.380
55236.59903	8.057	0.392
55241.55686	0.119	0.338
55243.55544	–2.422	0.222
55246.56091	–2.684	0.434
55247.55392	–1.318	0.411
55248.54372	10.235	0.357
HIRES 10-m Keck		
55221.76973	1.084	0.291
55221.81404	0.890	0.189
55221.82490	0.556	0.289
55221.89482	–0.232	0.220
55221.90689	–0.492	0.216
55221.97788	–1.869	0.353
55221.99025	–1.750	0.147
55222.98656	–3.193	0.340
55222.99752	–3.587	0.226
55223.73904	6.527	0.113
55224.82036	1.593	0.374
55224.83152	1.818	0.303
55225.04022	–1.345	0.515

These 3 spectra were coadded to serve as a stellar template for the RV measurements, and be used to determine the stellar parameters (see Sect. 4.3). Over a four-night run from 2010 January 25 to January 28, we collected 13 spectra of CoRoT-15 with the I_2-cell. The average SNRs of the spectra with the I_2-cell range from 13 to 22 (per pixel) in the iodine region from 500–620 nm. Differential radial velocities were computed using the *Austral* Doppler code (Endl et al. 2000). Nine RV measurements were obtained during a transit event on 2010 January 25 but they were not sensitive enough to detect the signature of the Rossiter-McLaughlin effect, which is expected to have, for this rapidly rotating star, an amplitude of about 100 m s^{-1}.

The HARPS and HIRES radial velocities are given in Table 2. The two sets of relative radial velocities were simultaneously fitted with a Keplerian model, both the epoch and period of the transit being kept fixed at the *CoRoT* value and there beeing an adjusted offset between the two different instruments. No significant eccentricity was found and we decided to set it to zero. We identified a systematic shift in phase using the *CoRoT* period of $P = 3.0608$ days, which originates in the fact that the quite large uncertainty in the *CoRoT* period (69 s) may introduce after one year a systematic shift of more than 2 h. When we adjust the period using the RVs while fixing the transit epoch to that determined from the *CoRoT* lightcurve $Tt = 54753.5570 \pm 0.0028$, the best-fit solution is found to correspond to $P = 3.06039 \pm 0.00014$ days and a semi-amplitude $K = 7.376 \pm 0.090$ km s^{-1}. The dispersion in the residuals is 0.325 km s^{-1} and the reduced χ^2 is 0.90. The joint analysis of the photometric and RV data, presented in Sect. 5, does not significantly change our results. Figure 3 shows all the radial velocity measurement after subtracting the RV offset and folding in phase with the updated orbital period.

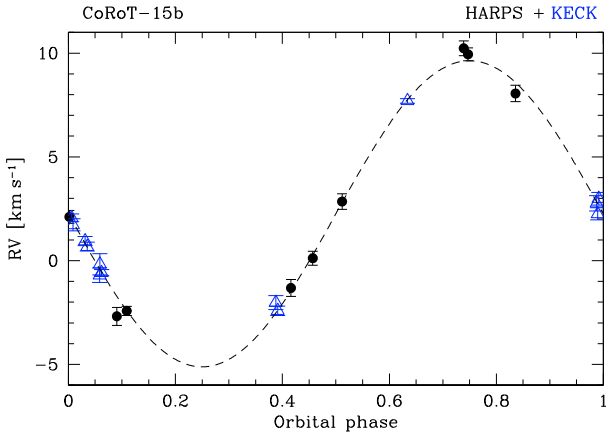

Fig. 3. Phase-folded radial velocity measurements of CoRoT-15 with HARPS (dark circle) and HIRES (open triangle).

4.3. Spectral classification

Three HIRES spectra of CoRoT-15 were acquired without the iodine cell. Each spectrum was shifted to the barycentric rest-frame, and cleaned of both cosmic rays and reflected moonlight. The co-addition of these three spectra results in a master spectrum covering the wavelength range from 4100 Å to 7800 Å with a SNR per element of resolution in the continuum ranging from 20 at 5300 Å up to 70 at 6820 Å. The nine co-added HARPS spectra unfortunately did not permit us to reach a higher SNR.

From the analysis of a set of isolated lines, we derived a $v \sin i$ of 19 ± 2 km s^{-1}. The spectroscopic analysis was carried out using the same methodology as for the previous *CoRoT* planets, which is described in detail in Bruntt et al. (2010). However, the moderate SNR of the master spectrum of this faint target, combined to the significant rotational broadening of the spectral lines prevented us from performing an accurate measurement of the star's photospheric parameters. The derived stellar parameters are reported in Table 3.

Following the methodology of Santos et al. (2002), we also estimated the $v \sin i$ and an [Fe/H] index from the HARPS cross-correlation average parameters (FWHM and surface). Assuming a $B - V$ of 0.5, we estimated the $v \sin i$ of the target to be 16 ± 1 km s^{-1} and an [Fe/H] index close to zero (solar metallicity) in agreement with the spectral analysis.

5. System parameters

The time span of the CoRoT light curve is relatively short, and the RV data were collected one year later. Jointly analysing the two datasets therefore yields significantly improved constraints on the period P and time-of-transit center $T_{\rm tr}$. We performed this joint analysis using a Metropolis-Hastings Markov Chain Monte Carlo (MCMC) algorithm (see Appendix 1 of Tegmark et al. 2004 for a general description of MCMC algorithms and Winn et al. 2008 and references therein for a detailed description of their application to transits). This has the added advantage of yielding full posterior probability distributions for the fitted parameters, ensuring that the effects of the well-known degeneracy between the orbital inclination i and system scale $a/R_\star$ (which leads to highly skewed probability distributions for these parameters, as well as for the radius ratio $R_{\rm c}/R_\star$) are properly taken into account in the final uncertainties.

Table 3. Star and companion parameters.

Parameters	Value
Transit epoch $T_{\rm tr}$ [HJD]	2454753.5608 ± 0.0011
Orbital period P [days]	3.06036 ± 0.00003
Transit duration $d_{\rm tr}$ [h]	3.24 ± 0.1
Orbital eccentricity e	0 (fixed)
Semi-amplitude K [km s^{-1}]	7.36 ± 0.11
Systemic velocity V_{0_harps} [km s^{-1}]	2.23 ± 0.11
Systemic velocity V_{0_hires} [km s^{-1}]	1.09 ± 0.07
Radius ratio $R_{\rm c}/R_\star$	$0.0788^{+0.0039}_{-0.0029}$
Scaled semi-major axis $a/R_\star$	$6.68^{+0.49}_{-1.04}$
Impact parameter[b]	$0.38^{+0.25}_{-0.26}$
$M_\star^{1/3}/R_\star$ [solar units]	$0.75^{+0.05}_{-0.12}$
Stellar density $\rho_\star$ [g cm^{-3}]	$0.60^{+0.13}_{-0.28}$
Inclination i [deg]	$86.7^{+2.3}_{-3.2}$
Effective temperature $T_{\rm eff}$ [K]	6350 ± 200
Surface gravity log g [dex]	4.3 ± 0.2
Metallicity [Fe/H] [dex]	0.1 ± 0.2
Rotationl velocity $v \sin i$ [km s^{-1}]	19 ± 2
Spectral type	F7V
Star mass [$M_\odot$]	1.32 ± 0.12
Star radius [$R_\odot$]	$1.46^{+0.31}_{-0.14}$
Distance of the system [pc]	1270 ± 300
Orbital semi-major axis[a] [AU]	$0.045^{+0.014}_{-0.010}$
Companion mass $M_{\rm c}$ [$M_{\rm Jup}$]	63.3 ± 4.1
Companion radius $R_{\rm c}$ [$R_{\rm Jup}$]	$1.12^{+0.30}_{-0.15}$
Companion density $\rho_{\rm c}$ [g cm^{-3}]	59^{+37}_{-32}
Equilibrium temperature $T_{\rm eq}^{\rm per}$ [K]	1740^{+120}_{-190}

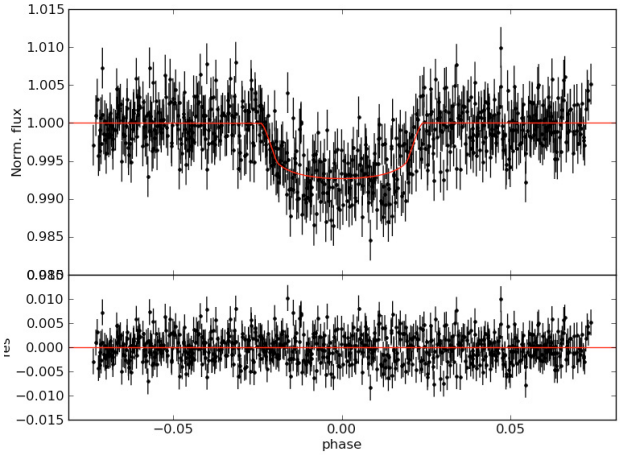

Fig. 4. Folded, detrended light curve of CoRoT-15 (*top*), showing the best-fit transit model (red solid line) and residuals (*bottom*).

The light curve was first pre-processed to remove out-of-transit variability as follows. Outliers were identified using an iterative non-linear filter (see Aigrain et al. 2009), and a straight line was fitted to the region around each transit. The effect of contamination reported in Sect. 4.1 was taken into account by subtracting a constant amount of flux equal to 1.9% of the mean flux from the light curve. Each section of the light curve was thus normalised, and a visual check was performed to ensure that no residual discontinuities affected the preprocessed light curve. The photometric uncertainties were then estimated from the out-of-transit scatter in the preprocessed light-curve section close to each transit. The light curve was modeled using the formalism of Mandel & Agol (2002). Given the relatively low SNR of the transits, we opted to fix the quadratic limb-darkening parameters u_a and u_b to the values given by Sing et al. (2010) for the star's effective temperature, gravity, and metallicity (adopted values: $u_a = 0.32$, $u_b = 0.30$). The RV data were modelled using a Keplerian orbit of eccentricity fixed at zero, since the data show no evidence of significant eccentricity. The relative zero-point of the HARPS and HIRES velocities, δV_0, was allowed to vary freely. The parameters of the MCMC were thus P, $T_{\rm tr}$, $R_{\rm c}/R_\star$, $a/R_\star$, the radial velocity semi-amplitude K, the systemic radial-velocity $V_{\rm sys}$, and δV_0.

After an initial chain of 10^5 steps to adjust the MCMC step sizes for each parameter, we performed 10 MCMC chains of 10^5 steps, each with different starting points. The convergence of the chains was checked using the Geldman-Rubin statistic (Geldman & Rubin 1992; Brooks & Geldman 1997). The chains were then combined (after discarding the first 10% of each chain, where the MCMC is settling from its starting point) to produce posterior probability distributions for each parameters. We report in Table 3 the median of the probability distribution for each parameter[2]. To estimate uncertainties for each parameter, we computed the range of values enclosing 68.5% of the probability distribution (by rejecting 16.25% at each extremum). Our uncertainties thus correspond to 68.5% confidence intervals, just as classical 1-σ uncertainties do for a Gaussian distribution. The best-fit transit model is shown superimposed on the folded light curve in Fig. 4. To highlight the correlations between b, $R_{\rm p}/R_\star$ and $a/R_\star$, and explain the rather large resulting uncertainties, we also show the posterior probability distributions and 2-D projections of the combined MCMC chain for these parameters in Fig. 5.

We used the photospheric parameters from the spectral analysis and the stellar density derived from the transit modeling to determine the star's fundamental parameters in the ($T_{\rm eff}$, $M_\star^{1/3}/R_\star$) space. Using *STAREVOL* evolution tracks (Palacios, priv. comm.), we find the stellar mass to be $M_\star = 1.32 \pm 0.10\, M_\odot$ and the stellar radius $R_\star = 1.46^{+0.31}_{-0.14}\, R_\odot$, with an age in the range 1.14–3.35 Gyr. This infers a surface gravity of $\log g = 4.23^{+0.12}_{-0.20}$, in good agreement with the spectroscopic value.

Calculations using CESAM (Morel & Lebreton 2008, see also Guillot & Havel 2010) confirm these solutions. The age constraints, 1.9 ± 1.7 Gyr, are however extremely weak, and yield possible pre-main sequence solutions with extremely young ages.

For the transiting companion, we derived $M_{\rm c} = 63.3 \pm 4.1\, M_{\rm Jup}$ and $R_{\rm c} = 1.12^{+0.30}_{-0.15}\, R_{\rm Jup}$.

6. Discussion and conclusions

CoRoT-15b is one of a rare type of transiting companion that lies in the theoretical mass domain of brown dwarfs (13–75 MJup, if one adopts the present IAU convention). In contrast to CoRoT-3b (Deleuil et al. 2008) that is located in the overlapping region between the massive planet and the brown-dwarf domain,

[2] The choice of which statistic to report is a somewhat tricky one. When the distributions are (close to) Gaussian, the median, most probable, and best-fit values coincide. When the distributions are skewed, as in the case of b for example, the median, most probable, and best-fit values can differ signficantly. Whilst the best-fit value maximises the merit function for the particular dataset being analysed, it has no special physical meaning. We adopt the value that divides the probability distribution into half, namely the median, as it is arguably the most physically meaningful.

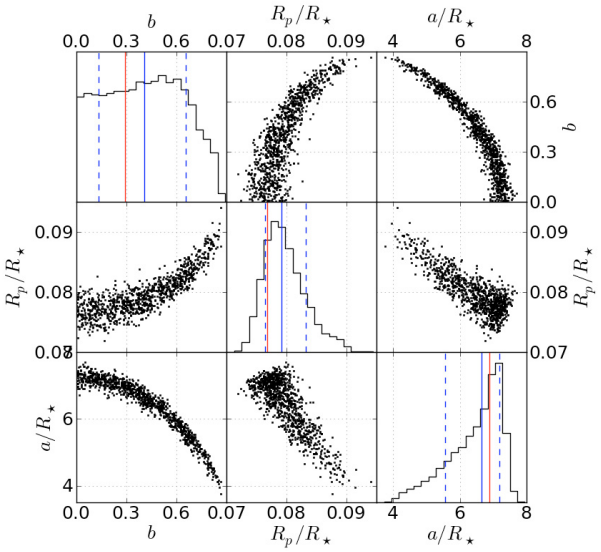

Fig. 5. Selected posterior probability distributions and two-dimensional correlations for the transit fit. The panels along the diagonal show single-parameter posterior probability distributions for b, $R_p/R_\star$, and $a/R_\star$. The red, blue, and dashed blue vertical lines indicate the location of the best-fit, median, and the limits of the 68.5% confidence interval for each parameter. The off-diagonal panels show, for each pair of parameters, scatter plots of 1000 points randomly selected from the combined MCMC chain. The density of the points approximates the joint posterior probability distribution.

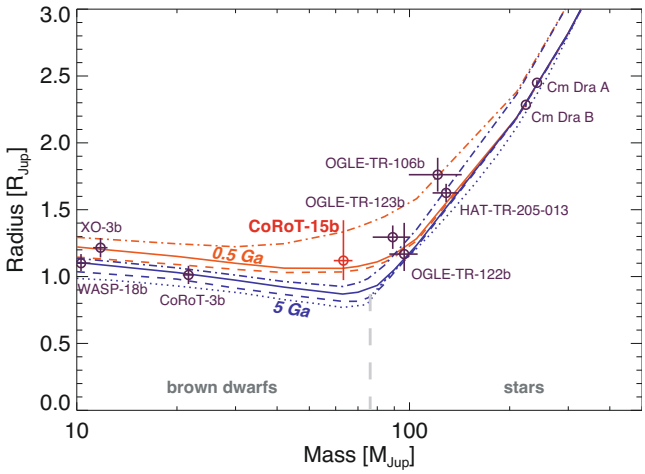

Fig. 6. Masses and radii of eclipsing brown-dwarfs and low-mass stars (circles with error bars, as labeled) compared to theoretical mass-radius relations (lines). The lines correspond to isochrones of 0.5 (upper orange lines) and 5 Ga (lower blue lines), respectively. The dashed lines are calculated for isolated brown-dwarfs and low-mass stars. The plain lines include the effect of irradiation with T_{eq} = 1800 K. The dash-dotted lines include irradiation and account for a 50% coverage of the photosphere with low-temperature spots (see text). A 5 Ga isochrone for isolated brown dwarfs/M stars from Baraffe et al. (2003) is shown for comparison (dotted line).

CoRoT-15b is well within the mass domain of BDs. If we were to slightly expand the mass domain, we could easily include in this ensemble the high-mass "planets" ($M \geq 10\ M_{Jup}$) XO-3b (Johns-Krull et al. 2008) and WASP-18b (Hellier et al. 2009), and in the M-dwarf regime, OGLE-TR-122b (Pont et al. 2005a), –123b (Pont et al. 2006), –106b (Pont et al. 2005b), and HAT-TR-205-013 (Beatty et al. 2007). Interestingly, all of these objects are found to orbit F-type stars (see also Deleuil et al. 2008), with one exception: OGLE-TR-122b orbits a G-type dwarf but has a much longer orbital period (7.3 days compared to less than 4.3 days for all other objects).

Early- and mid-F-type dwarfs are typically rapid rotators, independently of their age (Nordstrom et al. 1997), a consequence of a small or inexistent outer convective zone, weak stellar winds, and smaller losses of angular momentum. The tides raised on a star by its close-in companion (planet, brown dwarf, or star) have long been known to threaten its survival (e.g. Pätzold & Rauer 2002). This is true when the star's spin is slower than the orbital period of the companion, a common situation for close-in exoplanets. However, massive-enough companions have the possibility of spinning-up the star and may escape engulfment if the total angular momentum of the system is above a critical value (Levrard et al. 2009). Even in that case however, magnetic braking in the central star (e.g. see Barker & Ogilvie 2009) will lead to a loss of angular momentum that will be transferred to the orbit of the companion through tides and lead to orbital decay. We thus propose that close-in massive planets, brown dwarf or M-dwarf can survive when orbiting early or mid F-type dwarfs but be engulfed by G-type (or late F-type) dwarfs. In the case of CoRoT-15, we thus expect the star to be more massive than ~1.25 $M_\odot$ to avoid efficient spin-down, and that the system should be at or close to double-synchronisation (i.e. the spin period of the star should be close to the orbital period of its companion).

It is interesting to see that given the $v \sin i$ and stellar radius determinations, the projected spin period of the central star is $P/\sin i_* = 3.9^{+0.8}_{-1.1}$ days. An LS periodogram shows the presence of many peaks possibly due to low-level discontinuities in the lightcurve. The most robust peak compatible with the $v \sin i$ determination lies between 0.32 and 0.34 cycles/day, and may thus be linked to a stellar spin period between 2.9 and 3.1 days. The CoRoT-15 system thus appears to be indeed close to being double-synchronous. Additional observations of the system and in particular a precise determination of the stellar spin period would provide a powerful means of understanding the dynamical evolution of this system. Coupled to studies of similar systems, this may also yield strong constraints on the tidal dissipation factor in F-type dwarfs.

CoRoT-15b is also extremely interesting because of its size relative to other objects in this mass range, and the evolutionary tracks of hydrogen-helium brown dwarfs and stars. Figure 6 shows that it appears to be inflated compared to standard evolutionary tracks for these kind of objects (Baraffe et al. 2003), although it may be compatible with a young age if its true size is at the lower-end of the one inferred from our measurements. However, the same situation arises for OGLE-TR-123b, OGLE-TR-106b, and, but to a lesser extent, HAT-TR-205-013[3]. The two other known brown dwarfs with direct radius measurements, discovered in the 2MASS J05352184-0546085 eclipsing binary system (Stassun et al. 2006), have very large radii (5.0 and 6.5 R_{Jup}), but because of the very young age of the system (~1 Myr), are still in the earliest stages of gravitational contraction.

To examine solutions to this puzzle (other than there being a systematic overestimation of the inferred sizes for the

[3] The discovery of the transiting brown dwarf LHS6343C by Johnson et al. (2010) also appears to detect an inflated companion.

systems known thus far), we calculated evolutionary tracks using CEPAM (Guillot & Morel 1995), but adding the dominant thermonuclear reaction cycle, namely the pp-chain (see Burrows & Liebert 1993). The atmospheric boundary condition is adjusted to the Baraffe et al. (2003) evolutionary tracks, using the analytical solution of Guillot (2010), and values of the thermal and visible mean opacities, $\kappa_{\rm th} = 0.04$ cm^2 g^{-1} and κv = 0.024 cm^2 g^{-1}. The model shows that irradiation effects, although quite significant for Jupiter-like planets have rather small consequences in the brown dwarf regime, and become completely negligible in the stellar regime. We also tested the possibility that these inflated sizes may be explained by cold spots on the brown dwarf, as in the case of a mechanism proposed to explain that an M-type star in close-in binaries also appear inflated (Chabrier et al. 2007). As shown in Fig. 6, this mechanism works only in combination with a young age for the system, and with a rather large fraction (~50%) of the photosphere covered with spots. An alternative possibility is that irradiated atmospheres are much more opaque than usually thought, possibly a consequence of photochemistry and disequilibrium chemistry. A solar metallicity was assumed for the brown-dwarf models displayed in Fig. 6. We tested the effect of metallicity on the mean molecular mass and the opacity but did not find significant change in the radius.

In any case, this shows that CoRoT-15b is a crucial object to understand both the dynamical and physical evolution of giant planets, brown-dwarfs, and low-mass stars. Additional observations designed to acquire higher quality spectra of the star would be highly desirable. Although this would be a challenge given the faintness of the target, measurement of secondary transits in the infrared would be extremely interesting because they would provide us with insight into this rare heavily irradiated brown dwarf atmosphere.

Acknowledgements. The authors wish to thank the staff at ESO La Silla Observatory for their support and for their contribution to the success of the HARPS project and operation. HIRES data presented herein were obtained at the W.M. Keck Observatory from telescope time allocated to the NASA through the agency's scientific partnership with the California Institute of Technology and the University of California. The French team wish to thank the Programme National de Planétologie (PNP) of CNRS/INSU and the French National Research Agency (ANR-08-JCJC-0102-01) for their continuous support to our planet search program. The team at IAC acknowledges support by grant ESP2007– 65480-C02-02 of the Spanish Ministerio de Ciencia e Innovación. The German CoRoT Team (TLS and the University of Cologne) acknowledges DLR grants 50OW0204, 50OW0603, and 50QP07011. M.G. acknowledges support from the Belgian Science Policy Office in the form of a Return Grant. S.A. & N.G. acknowledge support from STFC standard grand ST/G002266. FB acknowledges the continuous support of PLS-230371.

References

Aigrain, S., Pont, F., Fressin, F., et al. 2009, A&A, 506, 425
Baglin, A., Auvergne, M., Barge, P., et al. 2009, Transiting Planets, Proceedings of the International Astronomical Union, IAU Symp., 253, 71
Baraffe, I., Chabrier, G., Barman, T. S., et al. 2003, A&A, 402, 701
Baranne, A., Queloz, D., Mayor, M., et al. 1994, A&AS, 119, 373
Barker, A., & Ogilvie, G. I. 2009, in Cosmic Magnetic Fields: From Planets, to Stars and Galaxies, Proceddings of the International Astronomical Union, IAU Symp., 259, 295
Beatty, T. G., Fernandez, J. M., Latham, D. W., et al. 2007, ApJ, 663, 573
Brooks, S. P., & Geldman, A. 1997, J. Comput. Graph. Stat., 7, 434
Bruntt, H., Deleuil, M., Fridlund, M., et al. 2010, A&A, 519, A51
Burrows, A., & Liebert, J. 1993, RvMP, 65, 301
Chabrier, G., Gallardo, J., & Baraffe, I. 2007, A&A, 472, L17
Deeg, H., Gillon, M., Shporer, A., et al. 2009, A&A, 506 343
Deleuil, M., Deeg, H., Alonso, R., et al. 2008, A&A, 491, 889
Endl, M., Kürster, M., & Els, S. 2000, A&A, 362, 585
Geem, Z. W., Kim, J. H., & Loganathan, G. V. 2001, Simulation, 76, 60
Gelman, A., & Rubin, D. B. 1992, Stat. Sci., 7, 457
Guillot, T., & Morel, P. 1995, A&AS, 109, 109
Guillot, T. 2010, A&A, 520, A27
Guillot, T., & Havel, M. 2010, A&A, accepted [arXiv:1010.1078]
Hellier, C., Anderson, D. R., Cameron, A. C., et al. 2009, Nature, 460, 1098
Johnson, J. A., Apps, K., Gazak, J. Z., et al. 2010, ApJ, submitted [arXiv:1008.4141]
Johns-Krull, C. M., McCullough, P. R., Burke, C. J., et al. 2008, ApJ, 677, 657
Levrard, B., Winisdoerffer, C., Chabrier, G., et al. 2009, ApJ, 692, L9
Llebaria, A., & Guterman, P. 2006, in ESA SP, 1306, 293
Mandel, K., & Agol, E. 2002, ApJ, 580, L171
Mayor, M., Pepe, F., Queloz, D., et al. 2003, The Messenger, 114, 20
Morel, P., & Lebreton, Y. 2008, Ap&SS, 316, 61
Nordstrom, B., Stefanik, R. P., Latham, D. W., et al. 1997, A&AS, 126, 21
Pätzold, M., & Rauer, H. 2002, ApJ, 568, L117
Pepe, F., Mayor, M., Galland, F., et al. 2002, A&A, 388, 632
Pont, F., Melo, C. H. F., Bouchy, F., et al. 2005a, A&A, 433, L21
Pont, F., Bouchy, F., Melo, C., et al. 2005b, A&A, 438, 1123
Pont, F., Moutou, C., Bouchy, F., et al. 2006, A&A, 447, 1035
Santos, N. C., Mayor, M., Naef, D., et al. 2002, A&A, 392, 215
Sing, D. K. 2010, A&A, 510, A21
Stassun, K. G., Mathieu, R. D., & Valenti, J. A. 2006, Nature, 440, 311
Surace, C., Alonso, R., Barge, P., et al. 2008, SPIE Conf. Ser., 7019, 111
Tegmark, M., Strauss, M. A., Blanton, M. R., et al. 2004, Phys. Rev. D, 69, 103501
Vogt, S. S., Allen, S. L., Bigelow, B. C., et al. 1994, SPIE, 2198, 362
Winn, J. N., Holman, M. J., Torres, G., et al. 2008, ApJ, 683, 1076

[1] Institut d'Astrophysique de Paris, UMR7095 CNRS, Université Pierre & Marie Curie, 98bis Bd Arago, 75014 Paris, France
e-mail: bouchy@iap.fr
[2] Observatoire de Haute Provence, CNRS/OAMP, 04870 St Michel l'Observatoire, France
[3] Laboratoire d'Astrophysique de Marseille, 38 rue Frédéric Joliot-Curie, 13388 Marseille Cedex 13, France
[4] Université de Nice-Sophia Antipolis, CNRS UMR 6202, Observatoire de la Côte d'Azur, BP 4229, 06304 Nice Cedex 4, France
[5] Department of Physics, Denys Wilkinson Building Keble Road, Oxford, OX1 3RH, UK
[6] Rheinisches Institut für Umweltforschung an der Universität zu Köln, Aachener Strasse 209, Köln 50931, Germany
[7] McDonald Observatory, The University of Texas, Austin, TX 78712, USA
[8] Instituto de Astrofosica de Canarias, 38205 La Laguna, Tenerife, Spain
[9] Departamento de Astrofísica, Universidad de La Laguna, 38200 La Laguna, Tenerife, Spain
[10] Observatoire de l'Université de Genève, 51 chemin des Maillettes, 1290 Sauverny, Switzerland
[11] LESIA, UMR 8109 CNRS, Observatoire de Paris, UPMC, Université Paris-Diderot, 5 place J. Janssen, 92195 Meudon, France
[12] Institut d'Astrophysique Spatiale, Université Paris XI, 91405 Orsay, France
[13] Institute of Planetary Research, German Aerospace Center, Rutherfordstrasse 2, 12489 Berlin, Germany
[14] University of Vienna, Institute of Astronomy, Türkenschanzstr. 17, 1180 Vienna, Austria
[15] IAG, University of Sao Paulo, Brazil
[16] Research and Scientific Support Department, ESTEC/ESA, PO Box 299, 2200 AG Noordwijk, The Netherlands
[17] Thüringer Landessternwarte, Sternwarte 5, Tautenburg 5, 07778 Tautenburg, Germany
[18] University of Liège, Allée du 6 août 17, Sart Tilman, Liège 1, Belgium
[19] Space Research Institute, Austrian Academy of Science, Schmiedlstr. 6, 8042 Graz, Austria
[20] School of Physics and Astronomy, Raymond and Beverly Sackler Faculty of Exact Sciences, Tel Aviv University, Tel Aviv, Israel
[21] Center for Astronomy and Astrophysics, TU Berlin, Hardenbergstr. 36, 10623 Berlin, Germany
[22] LUTH, Observatoire de Paris, CNRS, Université Paris Diderot, 5 place Jules Janssen, 92195 Meudon, France